Pramana – J. Phys. (2021) 95:114
https://doi.org/10.1007/s12043-021-02138-5

Proton shell closure in the superheavy region: Cluster radioactivity study in the isotopic set $^{270–318}118$

K PRADEEP KUMAR and K P SANTHOSH*

School of Pure and Applied Physics, Kannur University, Swami Anandatheertha Campus, Payyanur 670 327, India
*Corresponding author. E-mail: drkpsanthosh@gmail.com

MS received 8 February 2020; revised 1 March 2021; accepted 4 March 2021

Abstract. Cluster decay of the superheavy nuclei $^{270–318}118$ has been studied taking Coulomb and proximity potentials as interacting barriers. This study is based on the concept of cold valley. Cluster decay half-lives and other characteristics are computed for various clusters. The predicted α decay half-life values are compared with other theoretical models and also with the sole experimental value. Plots connecting half-lives with the neutron number of the daughter nuclei as well as with the neutron number of the parent nuclei, strongly indicated neutron shell closure at $N = 184$. Also, we noted that proton shell closure occurs at $Z = 114$. From our studies, we noted that the nuclide $^{298}_{184}114$, which is doubly closed, is very stable and we could reach the inference that $^{298}_{184}114$ is the most probable nuclide to be the centre of island of stability.

Keywords. Cluster decay; proton shell closure; centre of island of stability.

PACS Nos **23.70.+j; 23.60.+e; 27.90.+b**

1. Introduction

The spontaneous decay of nuclei with the emission of fragments heavier than α-particle is termed as cluster radioactivity. The phenomenon, which was predicted in the 1970s by Sandulescu *et al* [1] on the basis of quantum mechanical fragmentation theory (QMFT) [2], was confirmed in 1984 by Rose and Jones [3] in the radioactive decay of ^{14}C from ^{223}Ra. This rare cold, neutron less, process is intermediate between α decay and spontaneous fission. So far, about 30 such decays, with clusters ranging from ^{14}C to ^{34}Si [4] have been reported.

The knowledge of half-lives of different radioactive modes such as α decay and cluster decay can be used to decipher shell closures. Also, such half-lives along with fission half-lives are essential to identify the decay chains of superheavy elements, which are the experimental signatures of the formation of superheavy elements in fusion reactions.

The existence of superheavy nuclei (the trans actinides), with $Z \geq 104$, is due to quantum shell effects, and pronounced shell gaps stabilise the nuclei. The existence of an island of stability of long-lived superheavy elements in the vicinity $Z = 126$, $N = 184$ had been predicted by various theoretical studies [5,6] in the 1960s. Yet, later, some other calculations, mainly in the self-consistent mean field, predicted the next double closed shell nucleus to be with $Z = 114$, 120 or 126 with $N = 184$ [7–9]. Self-consistent models also indicated that the occurrence of a spherical proton (neutron) shell closure with the given $Z(N)$ can change with varying neutron number N (proton number Z) [10].

In the present work, attempt is made to examine, on a theoretical footing, the cluster emission from nuclei in the superheavy region with an aim to find proton shell closures, with stress on the superheavy region, which, in turn, shall give indication on the island of stability in the superheavy region.

Within Coulomb and proximity potential model [11–14], we have studied cluster emission from all even–even nuclei $^{270}118$, $^{272}118$, ... ,$^{316}118$, $^{318}118$ which are 25 isotopes in number. We have studied cold valleys and computed α decay half-life values and cluster decay half-life values for these nuclei. We studied the emission of clusters up to ^{44}S.

Published online: 05 July 2021

2. The model

The interacting potential barrier for a parent nucleus exhibiting exotic decay is given by

$$V = \frac{Z_1 Z_2}{r} e^2 + V_{\rm p}(z) + \frac{\hbar^2 l(l+1)}{2\mu r^2}, \text{ for } z > 0. \quad (1)$$

Here Z_1 and Z_2 are the atomic numbers of the daughter and the emitted cluster, r is the distance between fragment centres, l is the angular momentum, μ is the reduced mass and $V_{\rm p}(z)$ is the proximity potential with z the smallest distance between the fragment surfaces, given by Blocki *et al* [15]

$$V_{\rm p}(z) = 4\pi\gamma b \left[\frac{C_1 C_2}{(C_1 + C_2)}\right] \phi\left(\frac{z}{b}\right) \quad (2)$$

with the nuclear surface tension coefficient,

$$\gamma = 0.9517[1 - 1.7826(N - Z)^2/A^2]\ \text{MeV/fm}^2, \quad (3)$$

where N, Z and A represent neutron, proton and mass number of the parent. The universal proximity potential Φ is given as [16]

$$\Phi(\varepsilon) = -4.41 e^{-\varepsilon/0.7176}, \text{ for } \varepsilon \geq 1.9475 \quad (4)$$

$$\Phi(\varepsilon) = -1.7857 + 0.9270\varepsilon + 0.0169\varepsilon^2 - 0.05148\varepsilon^3, \text{ for } 0 \leq \varepsilon \leq 1.947 \quad (5)$$

with $\varepsilon = z/b$, where the width (diffuseness) of the nuclear surface $b \approx 1$ and Sussmann central radii C_i of the fragments, the related to sharp radii R_i, is

$$C_i = R_i - (b^2/R_i). \quad (6)$$

For R_i we use the semiempirical formula in terms of mass number A_i as [15]

$$R_i = 1.28A_i^{1/3} - 0.76 + 0.8A_i^{-1/3}. \quad (7)$$

For the pre-scission phase of the decay process, the potential between the parent part and the cluster part is given by the Coulomb and proximity potential model, as

$$V = a_0(L - L_0)^n \text{ for } z < 0. \quad (8)$$

Here $L = z + 2C_1 + 2C_2$ and $L_0 = 2C$, the diameter of the parent nuclei. The constants a_0 and n are determined by the smooth matching of the two potentials at the touching point.

Using one-dimensional WKB approximation, the barrier penetrability P is given as

$$P = \exp\left\{-\frac{2}{\hbar}\int_a^b \sqrt{2\mu\,(V - Q)}\,{\rm d}z\right\}. \quad (9)$$

Here the mass parameter is replaced by $\mu = mA_1A_2/A$, where m is the nucleon mass and A_1, A_2 are the mass numbers of the daughter and the emitted cluster respectively.

The turning points a and b are given by $V(a) = V(b) = Q$, where Q is the energy released during the reaction which, alternatively, is known as decay energy of the reaction or Q-value. Q-value in a decay is fully utilised as the kinetic energy of the constituents. The above integral can be evaluated numerically or analytically.

The half-life time of a decay is given by

$$T_{1/2} = \ln 2/\lambda = \ln 2/\nu P, \quad (10)$$

where λ is the decay constant and $\nu = \omega/2\pi = 2E_v/h$ is the number of assaults on the barrier per second. E_v, the empirical zero-point vibration energy, is given as [17]

$$E_v = Q\left\{0.056 + 0.039 \exp\left[\frac{4 - A_2}{2.5}\right]\right\}, \text{ for } A_2 \geq 4. \quad (11)$$

3. Results and discussion

We studied the cluster radioactivity based on the potential barrier (or interaction potential) determined by two-sphere approximation, which is the sum of Coulomb ($V_{\rm C}$) and proximity ($V_{\rm p}$) potentials, for the touching and separated configurations.

The possibility to have a cluster decay process is

$$Q = M(A, Z) - M(A_1, Z_1) - M(A_2, Z_2) > 0, \quad (12)$$

where $M(A,\ Z), M(A_1,\ Z_1), M(A_2,\ Z_2)$ are the atomic masses of the parent, daughter and cluster respectively. The quantity, driving potential ($V_{\rm d}$), is defined as the difference between the interaction potential and the decay energy (Q-value) of the reaction.

Q-values are computed mainly using experimental mass excess of Audi and Wapstra [18]. Some values are taken from the mass table of Koura *et al* [19] and in a few cases data from the finite-range droplet model [20] are used. So, full shell effects are contained in our calculation that comes from experimental and/or calculated binding energies.

Driving potential of the compound nucleus is calculated as a function of mass and charge asymmetries

$$\eta_A = \frac{A_1 - A_2}{A_1 + A_2} \quad \text{and} \quad \eta_Z = \frac{Z_1 - Z_2}{Z_1 + Z_2}$$

for the touching configuration of the fragments. Or, the driving potential of the compound nucleus is calculated for all sensible, possible cluster–daughter combinations

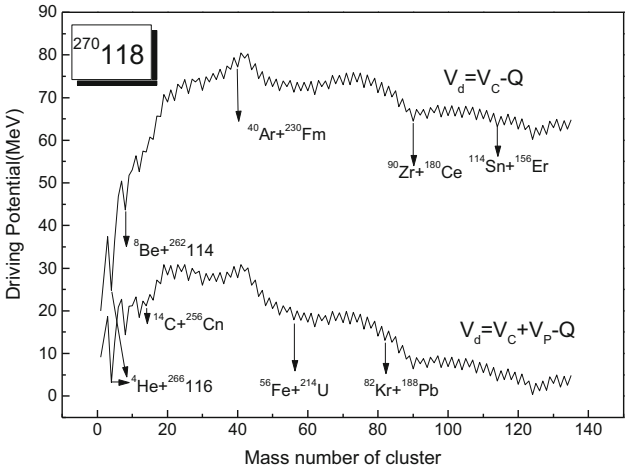

Figure 1. Plots of driving potential vs. mass number of the cluster for ^{270}118 isotope for the touching configuration, $r = C_1 + C_2$.

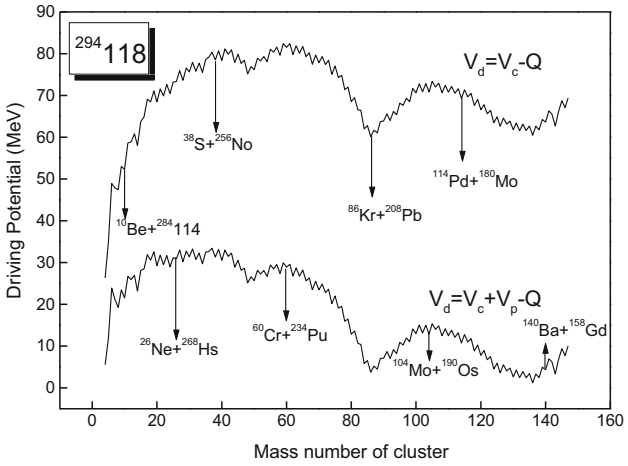

Figure 2. Plots of driving potential vs. mass number of the cluster for ^{294}118 isotope for the touching configuration, $r = C_1 + C_2$.

for the touching configuration. In the touching configuration, the distance between the fragments $r = C_1 + C_2$ where C_1 and C_2 are the Sussman central radii. For a fixed η_A and r the charges of the fragments are fixed by minimising the driving potential, i.e. for a fixed pair of masses in the mass asymmetric coordinate, a fixed pair of charges is pin-pointed out from the charge asymmetric coordinate such that the driving potential involved is minimum. In that way, for every fixed pair of masses, a single pair of charges is pin-pointed out from the corresponding charge asymmetric coordinate. Meanwhile, a set of driving potential minimum is evolved.

The driving potential minimum represents the most probable decay for a particular pair of (A_1, A_2) and is made use of for further analysis. The concept of cold valley was introduced in relation to the structure of the set of driving potential minimum. The set of driving potential minimum itself contains, alternatively, maxima and minima. Minimum in the set of driving potential minimum is known as the cold valley. The reaction depicted by cold valley has more probability to occur than that by the adjacent maxima. A cold valley represents the most probable reaction of successive few pairs of (A_1, A_2).

An improved model of proximity potential, that was used originally by Shi and Swiatecki [21] and thereafter by Malik and Gupta [22], has been used in the present model. Here, another formulation of proximity potential [16] as given in eqs (4) and (5) is used. Here, assault frequency ν, which is associated with zero-point vibration energy, is calculated for each parent–cluster combination. But, Shi and Swiatecki [21] used rather unrealistic values (10^{22} for even A parent and 10^{20} for odd A parent).

The angular momentum l carried in the cluster decay process, appearing in eq. (1) is very small ($\approx 5\hbar$) and its contribution to half-life is shown to be small [11–14,17]. In the present work, calculations are done assuming zero angular momentum transfers.

Figures 1–3 are the plots of driving potential minimum vs. mass of one of the fragments, the cluster A_2, for the isotopes ^{270}118, ^{294}118 and ^{318}118 by including and excluding proximity potential. (These plots are presented as representatives of the 25 plots for the set of isotopes $^{270-318}$118). The plots, which are essentially constituted by maxima and minima, contain some sagged regions (which are generally mentioned as 'troughs' by the author, two of which are known already as mass-asymmetry valleys), due to the shell effects of one or both fragments. Inclusion of proximity potential reduces height of the barrier, which agrees well with the experiment. From figure 1 it can be seen that, in addition to α-particles, ^{1}P, ^{8}Be, ^{12,14}C, ^{16,18}O, ^{20,22}Ne, $^{24-26}$Mg clusters are most probable for emission from ^{270}118. It was noted that though, for a fixed pair (A_1, A_2), there exists a fixed pair (Z_1, Z_2) with the minimum driving potential, there are many pairs of (A_1, A_2) having the same pair of (Z_1, Z_2).

The dynamical quantity, the half-life, in principle depends not only on nuclear structure but also on nuclear inertia. The half-life is relied upon for finding the stability of each of ^{270}118 to ^{318}118 parent nuclei against each cluster emission. The parent nuclei with $T_{1/2} > 10^{30}$ s are generally stable against cluster decay. It is found that half-life has minimum value for those decays which lead to the doubly magic daughter [23]. By simple logic, this statement can be generalised as: half-life has minimum value for those decays which involve doubly magic

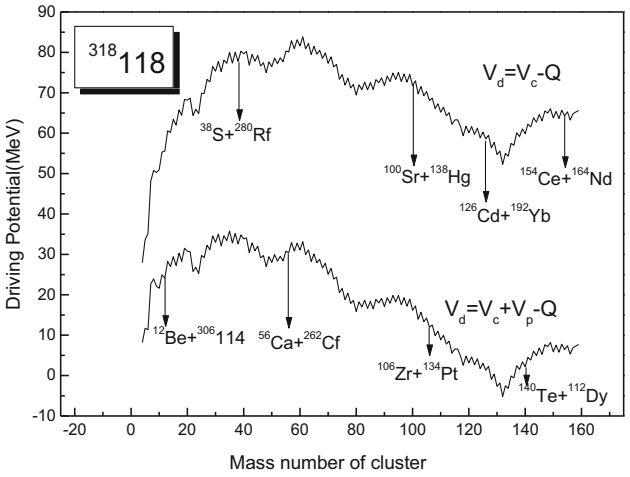

Figure 3. Plots of driving potential vs. mass number of the cluster for $^{318}118$ isotope for the touching configuration, $r = C_1 + C_2$.

daughter or doubly magic cluster. And some parallel variations based on a combination of aspects, namely, daughter is doubly magic, daughter is singly magic, cluster is doubly magic, cluster is singly magic can be thought of.

The plot of driving potential minima vs. mass number of the cluster, as mentioned earlier, contains maxima and minima (cold valleys). Using the values embedded with minimum, half-life of the associated reaction is calculated.

Half-life of each of the most probable reactions of $^{270}118$ is found. This is done, also, for all the members of the isotopic sub-set $^{272–318}118$. Half-life of clusters ^{1}P, ^{4}He, ^{8}Be, ^{10}Be, ^{12}C, ^{14}C, ^{16}C, ^{18}C, ^{16}O, ^{18}O, ^{20}O, ^{22}O, ^{24}O, ^{20}Ne, ^{22}Ne, ^{24}Ne, ^{26}Ne, ^{28}Ne, ^{24}Mg, ^{26}Mg, ^{28}Mg, ^{30}Mg, ^{32}Mg, ^{30}Si, ^{32}Si, ^{34}Si, ^{36}Si, ^{38}S, ^{40}S, ^{42}S, ^{44}S are calculated.

In a strict sense, ^{1}P is not a cluster. But cluster emission is related to certain concepts and laws rather than to a particular mass number or neutron number and hence, emission of ^{1}P can come under the purview of cluster emission. Only these clusters are emitted, as emissions of other clusters, say ^{20}C, are either energetically, as warranted by the concepts of cluster emission, are impossible or their probability of emission are very low tending to zero. In connection with emission from members of the isotopic set $^{270–318}118$, all clusters are not emitted from all isotopes. Generally, some sets of clusters are emitted from some isotopes; whereas some other sets of clusters are emitted from some other isotopes. Also it is noted that some clusters are emitted, almost, throughout the range.

The sub-set $^{270–280}118$ is neutron-deficient. (The terms neutron-deficient, neutron-sufficient synonymous to approximately equal number of neutrons and protons, and neutron-rich are used, to enhance consistency in terminology). As a result, comparatively, acutely neutron-deficient or neutron-deficient clusters are emitted from this range. This gives the reason for the emission of ^{1}P, ^{4}He, ^{8}Be etc. from this range. Also, clusters like ^{44}S which are neutron-rich are not emitted from these isotopes. As we go up from $^{280}118$ to isotopes of higher neutron value to reach neutron-sufficient isotopes, like $^{290}118$, clusters like ^{20}O which are neutron-sufficient, are emitted. Emission of ^{1}P ceases. When we go up from $^{290}118$ to reach neutron-rich isotope $^{310–318}118$, neutron-rich clusters like ^{32}Mg, ^{38}Si, ^{44}S are emitted. Generally, from a given type of parent, same types of clusters alone are emitted. Of the 10 clusters which are emitted from $^{270}118$, only 2 clusters, namely, ^{4}He and ^{14}C, are emitted from $^{318}118$.

^{4}He and ^{14}C are found to emit from neutron-deficient, neutron-sufficient, neutron-rich isotopes. Emission of ^{4}He shows that the combination of two protons, when supported by two neutrons, becomes very strong. The cohesion among them is so strong that, the group can withstand extreme neutron imbalanced environment. And as the combination does come outside from all the nuclides, it may be inferred that it is more responsive to proton environment, than to neutron environment. Emission of ^{14}C shows that the combination of eight protons is very strong (combination of six neutrons, on the other hand, may not be as strong as combination of eight protons because ^{12}C which also contains six neutrons was emitted from $^{270}118$ through $^{296}118$, only).

Parameters like Q-value, penetrability, decay constant and logarithmic half-life for all the emitted particles from each of the isotopes are found out. Tables 1–3 give these quantities for the isotopes $^{270}118$, $^{294}118$ and $^{318}118$. (These tables are presented as representatives of the 25 tables for the set of isotopes $^{270–318}118$.) The α-decay half-life of $^{294}118$ is found to be $0.89^{+1.07}_{-0.31} \times 10^{-3}$ s [24], and in some other works by the same authors where production of $^{294}118$ is mentioned, half-life is found to be $1.8^{+75}_{-1.3} \times 10^{-3}$ s [25], Q-value being 11.65 MeV. Present α-decay half-life value is 1.23×10^{-1} s, Q-value being 11.17 MeV. Our calculated value of half-life agrees within two orders of magnitude with the experimental value. In the present study, both emitted cluster and daughter nuclei are treated as spherical, and if we incorporate quadrupole (β_2) and hexadecapole (β_4) deformations of interacting nuclei, it will modify the barrier and will give better results that are close to the experimental value. The experimental value $\log_{10}(T^{\alpha}_{1/2}) = -3.05^{+0.34}_{-0.19}$ [24] is given in the last column of table 2.

Table 1. The computed half-life values, barrier penetrability and other characteristics of the isotope $^{270}118$ with zero angular momentum transfers. Masses are taken from [18–20].

Parent nuclei	Emitted cluster	Daughter nuclei	Q-value (MeV)	Penetrability P	Decay constant	$\log_{10}T_{1/2}$ (s)
$^{270}118$	^{1}p	$^{269}117$	0.911	1.163e-39	9.506e-20	18.86
	^{4}He	$^{266}116$	13.72	2.684e-15	1.691e+06	−6.39
	^{8}Be	$^{262}114$	27.93	1.610e-29	1.389e-08	7.70
	^{12}C	$^{258}112$	49.16	1.063e-31	1.455e-10	9.68
	^{14}C	$^{256}112$	43.13	1.608e-42	1.903e-61	20.56
	^{16}O	$^{254}110$	69.59	8.194e-36	1.553e-14	13.65
	^{18}O	$^{252}110$	62.77	2.455e-46	1.484e-25	24.22
	^{20}Ne	$^{250}108$	86.98	6.945e-44	1.638e-22	21.63
	^{22}Ne	$^{248}108$	85.26	5.613e-46	2.997e-24	23.73
	^{24}Mg	$^{246}106$	108.36	8.201e-46	2.407e-24	23.46
	^{26}Mg	$^{244}106$	108.09	2.879e-45	8.427e-24	22.92

Table 2. The computed half-life values, barrier penetrability and other characteristics of the isotope $^{294}118$ with zero angular momentum transfers. Masses are taken from [18–20].

Parent nuclei	Emitted cluster	Daughter nuclei	Q-value (MeV)	Penetrability P	Decay constant	$\log_{10}T_{1/2}$ (s)	
						Present	Expt. [24]
$^{294}118$	^{4}He	$^{290}116$	11.17	1.119e-20	5.738	−0.91	$-3.05^{+0.34}_{-0.19}$
	^{8}Be	$^{286}114$	22.31	4.471e-41	3.081e-20	19.35	
	^{10}Be	$^{284}114$	16.13	1.766e-66	8.203e-46	44.93	
	^{12}C	$^{282}112$	40.37	1.885e-45	2.119e-24	23.51	
	^{14}C	$^{280}112$	39.89	9.008e-48	9.855e-27	25.85	
	^{16}C	$^{278}112$	31.76	5.480e-71	4.740e-50	49.17	
	^{18}O	$^{276}110$	56.74	3.038e-55	4.681e-34	33.17	
	^{20}O	$^{274}110$	55.46	1.569e-58	2.359e-37	36.47	
	^{22}O	$^{272}110$	52.94	7.600e-65	1.090e-43	42.80	
	^{24}Ne	$^{270}108$	79.03	3.878e-53	8.301e-32	30.92	
	^{28}Mg	$^{266}106$	99.83	8.561e-54	2.315e-32	31.48	
	^{30}Mg	$^{264}106$	96.64	1.239e-58	3.242e-37	36.33	
	^{32}Si	$^{262}104$	120.20	7.707e-55	2.509e-33	32.44	
	^{34}Si	$^{260}104$	119.32	2.705e-55	8.741e-34	32.90	
	^{38}S	$^{256}102$	137.55	8.191e-59	3.051e-37	36.36	
	^{40}S	$^{254}102$	136.65	4.012e-59	1.485e-37	36.67	

It is found that, of all the most probable clusters, ^{4}He, ^{8}Be, ^{12}C, ^{14}C, ^{18}O, ^{22}Ne, ^{28}Mg are even more probable for emission with half-life, $T_{1/2} < 10^{30}$ s. Reaction in which one fragment is α-particle, is having minimum half-life in all the isotopes. This is due to the high stability of α-particle rather than due to any peculiar feature of the parent isotope or the daughter nuclide. Alpha particle which contains 2 protons and 2 neutrons has neutron and proton shell closures.

Since it has been found that half-life has minimum value for those cluster decays which lead to doubly magic daughter [23], it can be reasonably inferred that, those cluster decays which consistently have second-minimum half-life, leads to (singly) magic daughter. This inference shall be especially right when the cluster involved in the decay, as such, is not a magic one (but, a general one).

Table 4 gives the first and second least half-lives (and in some special cases third also) for each member of the isotopic set $^{270–318}118$. In isotopes $^{270}118$, $^{274–296}118$, $^{300–304}118$, emission of ^{8}Be has the second least half-life. In $^{298}118$, $^{306–314}118$ emission of ^{14}C has the second least half-life. In $^{316–318}118$, emission of ^{22}O has the second least half-life. In $^{272}118$, ^{1}P has the second least half-life. In all, sixteen Be nuclei, six C nuclei and two O nuclei have the second least half-life, out of the 25 isotopes. The reactions with second least half-life are as follows: In $^{270}118$,

Table 3. The computed half-life values, barrier penetrability and other characteristics of the isotope $^{318}118$ with zero angular momentum transfers. Masses are taken from [18–20].

Parent nuclei	Emitted cluster	Daughter nuclei	Q-value (MeV)	Penetrability P	Decay constant	$\log_{10}T_{1/2}$ (s)
$^{318}118$	^{4}He	$^{314}116$	8.58	1.130e-28	4.450e-08	7.19
	^{10}Be	$^{308}114$	15.89	6.935e-67	3.173e-46	45.34
	^{12}Be	$^{306}114$	10.23	2.412e-112	6.875e-92	91.00
	^{14}C	$^{304}112$	35.42	3.002e-57	2.916e-36	35.35
	^{16}C	$^{302}112$	32.46	1.173e-67	1.037e-46	45.83
	^{18}C	$^{300}112$	29.02	6.880e-42	5.421e-61	60.11
	^{22}O	$^{296}110$	55.69	5.007e-57	7.555e-36	34.96
	^{24}O	$^{294}110$	54.19	7.200e-61	1.057e-39	38.82
	^{26}Ne	$^{292}108$	75.18	3.618e-58	7.368e-37	35.97
	^{28}Ne	$^{290}108$	71.28	3.556e-66	6.866e-45	44.00
	^{30}Mg	$^{288}106$	93.12	1.583e-62	3.991e-41	40.24
	^{32}Mg	$^{286}106$	92.18	5.726e-64	1.429e-42	41.69
	^{34}Mg	$^{284}106$	89.14	1.073e-69	2.591e-48	47.43
	^{36}Si	$^{282}104$	112.13	6.774e-64	2.057e-42	41.53
	^{38}Si	$^{280}104$	110.71	7.833e-66	2.349e-44	43.47
	^{40}S	$^{278}102$	130.56	4.216e-66	1.491e-44	43.67
	^{42}S	$^{276}102$	132.44	9.326e-62	3.345e-40	39.32
	^{44}S	$^{274}102$	130.51	3.003e-64	1.061e-42	41.81

Table 4. The computed least two half-life values (and in some special cases third also), barrier penetrability and other characteristics for each of the isotopes of $^{270-318}118$.

Parent nuclei	Emitted cluster	Daughter nuclei	Q-value (MeV)	Penetrability P	Decay constant	$\log_{10}T_{1/2}$ (s)		
						Present	[28]	[30]
$^{270}118$	^{4}He	$^{266}116$	13.72	2.684e-15	1.691e+06	−6.39		
	^{8}Be	$^{262}114$	27.93	1.610e-29	1.389e-08	7.70		
$^{272}118$	^{1}p	$^{271}117$	1.68	8.074e-26	1.218e-05	4.76		
	^{4}He	$^{268}116$	14.70	2.040e-13	1.377e+08	−8.30		
	^{8}Be	$^{264}114$	28.72	5.876e-28	5.213e-07	6.12		
$^{274}118$	^{4}He	$^{270}116$	14.62	1.613e-13	1.083e+08	−8.19		
	^{8}Be	$^{266}114$	28.50	2.826e-28	2.487e-07	6.44		
$^{276}118$	^{4}He	$^{272}116$	14.40	7.046e-14	4.660e+07	−7.83		
	^{8}Be	$^{268}114$	28.19	9.080e-29	7.906e-08	6.94		
$^{278}118$	^{4}He	$^{274}116$	14.27	5.395e-17	35355	−7.62		
	^{8}Be	$^{270}114$	27.86	2.478e-35	2.132e-14	7.49		
$^{280}118$	^{4}He	$^{276}116$	14.13	2.645e-14	1.72e+07	−7.39		
	^{8}Be	$^{272}114$	27.52	6.953e-30	5.91e-09	8.07		
$^{282}118$	^{4}He	$^{278}116$	12.94	1.160e-16	68936.9	−5.00		−4.69
	^{8}Be	$^{274}114$	26.20	1.864e-32	1.508e-11	10.66		
$^{284}118$	^{4}He	$^{280}116$	12.75	4.887e-17	28615.9	−4.62		−4.26
	^{8}Be	$^{276}114$	25.62	1.326e-33	1.049e-12	11.82		
$^{286}118$	^{4}He	$^{282}116$	12.34	6.370e-18	3609.58	−3.72		−3.69
	^{8}Be	$^{278}114$	24.68	1.341e-35	1.022e-14	13.83		
$^{288}118$	^{4}He	$^{284}116$	11.91	6.681e-19	365.414	−2.72		−2.40
	^{8}Be	$^{280}114$	23.63	5.639e-38	4.115e-17	16.23		
$^{290}118$	^{4}He	$^{286}116$	11.65	1.658e-19	88.6988	−2.11	−2.52	−2.43
	^{8}Be	$^{282}114$	22.73	3.939e-40	2.765e-19	18.40		
$^{292}118$	^{4}He	$^{288}116$	11.47	6.282e-20	33.088	−1.68	−2.13	−1.75
	^{8}Be	$^{284}114$	22.21	2.087e-41	1.432e-20	19.68		

Table 4. *Continued.*

Parent nuclei	Emitted cluster	Daughter nuclei	Q-value (MeV)	Penetrability P	Decay constant	$\log_{10}T_{1/2}$ (s)		
						Present	[28]	[30]
$^{294}118$	^{4}He	$^{290}116$	11.17	1.119e-20	5.738	−0.91		−0.88
	^{8}Be	$^{286}114$	22.31	4.471e-41	3.081e-20	19.35		
$^{296}118$	^{4}He	$^{292}116$	11.95	1.134e-18	622.395	−2.95	−2.86	−1.05
	^{8}Be	$^{288}114$	22.56	2.321e-40	1.618e-19	18.63		
$^{298}118$	^{4}He	$^{294}116$	11.12	9.536e-21	4.870	−0.85	−1.37	−1.83
	^{14}C	$^{284}112$	39.55	2.605e-48	2.826e-27	26.39		
$^{300}118$	^{4}He	$^{296}116$	11.04	6.239e-21	3.163	−0.66	−1.20	−1.31
	^{8}Be	$^{292}114$	26.448	5.530e-44	3.622e-23	21.49		
$^{302}118$	^{4}He	$^{298}116$	10.92	3.150e-21	1.579	−0.36	−0.93	
	^{8}Be	$^{294}114$	21.088	3.867e-44	2.519e-23	22.44		
$^{304}118$	^{4}He	$^{300}116$	12.44	2.095e-17	11969	−4.24	−4.45	
	^{8}Be	$^{296}114$	22.48	2.585e-40	1.795e-19	18.59		
$^{306}118$	^{4}He	$^{302}116$	11.90	1.213e-18	662.781	−2.98		
	^{14}C	$^{292}112$	41.08	1.233e-44	1.390e-23	22.70		
$^{308}118$	^{4}He	$^{304}116$	11.30	4.010e-20	20.807	−1.48		
	^{14}C	$^{294}112$	41.92	8.301e-43	9.544e-22	20.86		
$^{310}118$	^{4}He	$^{306}116$	10.28	5.963e-23	0.028	1.39		
	^{14}C	$^{296}112$	42.07	2.053e-42	2.369e-21	20.47		
$^{312}118$	^{4}He	$^{308}116$	9.28	3.672e-26	1.565e-05	4.65		
	^{14}C	$^{298}112$	39.88	6.122e-47	6.697e-26	25.01		
$^{314}118$	^{4}He	$^{310}116$	9.04	5.458e-27	2.266e-06	5.49		
	^{14}C	$^{300}112$	37.92	2.777e-51	2.889e-30	29.38		
$^{316}118$	^{4}He	$^{312}116$	8.82	9.908e-28	3.608e-07	6.28		
	^{22}O	$^{294}110$	57.30	1.248e-53	1.937e-32	31.55		
$^{318}118$	^{4}He	$^{314}116$	8.58	1.130e-28	4.450e-08	7.19		
	^{22}O	$^{296}110$	55.69	5.007e-57	7.555e-36	34.96		

the reaction involved is ^{8}Be $+^{262}114$; in $^{274–296}118$ the reactions are ^{8}Be $+^{266–288}114$; in $^{300–304}118$ the reactions are ^{8}Be $+^{292–296}114$; in $^{306–314}118$ the reactions are ^{14}C $+^{292–300}$Cn; in $^{316–318}118$ the reactions are ^{22}O$+^{294–296}$Ds.

In the case of α-decay, for $^{284}118$, the present work gives $\log_{10}(T^{\alpha}_{1/2}/\text{s}) = -4.62$ (or, $T_{1/2} = 2.40\times10^{-5}$ s). Bhuyan *et al* [26], using Skirme Hartree–Fock (SHF) with SkI4 parameter, obtained $\log_{10}(T^{\alpha}_{1/2}/\text{s}) = -9.11$ (or, $T_{1/2} = 7.76 \times 10^{-10}$ s). Same researchers, using relativistic mean field (RMF) with NL3 parameter set obtained $\log_{10}(T^{\alpha}_{1/2}/\text{s}) = -5.48$ (or, $T_{1/2} = 3.31 \times 10^{-6}$ s) [26]. Moller *et al* [20,27], using finite-range droplet model, obtained $\log_{10}(T^{\alpha}_{1/2}/\text{s}) = -4.08$ (or, $T_{1/2} = 8.32 \times 10^{-5}$ s).

The predicted half-life values for the emission of ^{4}He are compared with the values reported by Cui *et al* [28] using effective liquid drop model (ELDM), where they used Q values computed using the mass tables of Koura *et al* [19], but in the case of $^{296}118$, WS4 mass tables [29] are used. Our values of ^{4}He emissions are also compared with the values of Sayahi *et al* [30] using density-dependent nuclear potential, the Paris M3Y parametrisation. From table 4, it can be seen that our predicted values are in agreement with these model predictions.

Clusters belonging to Be have the second-least half-life in most of the isotopes. Of the 17 isotopes from which ^{8}Be emission takes place, emission of ^{8}Be has the second-least half-life in 16. We cannot attribute this to strong cohesive force among the four protons involved. We can only attribute this to the peculiar nature of the daughter nuclei. Daughter nuclei have atomic number 114. This implies 114 protons make a strong combination or shell closure occurs at proton number 114. On the basis of the preformed cluster model, Gupta *et al* [31], by α decay method, found that there is an indication of proton magicity at $Z = 114$.

^{14}C has the second-least half-life in six isotopes. But here, the cluster contains magic neutron number 8. Hence, second-leastness can be attributed only to this. It cannot be used to assign magicity to atomic number 112 of the daughter nuclei in the way it is done in the

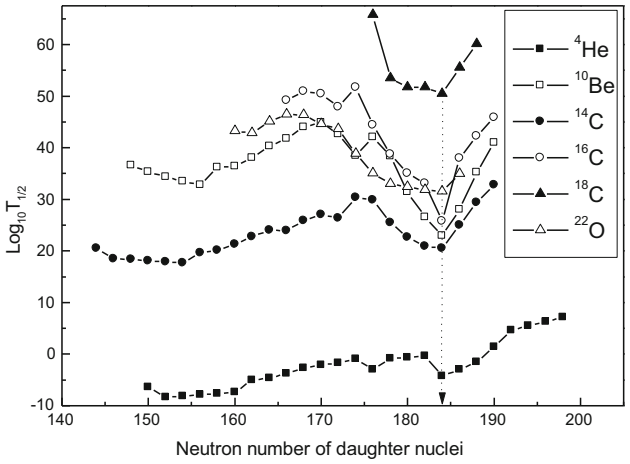

Figure 4. Computed half-life vs. neutron number of the daughter nuclei for the parent Z = 118. The plots have the minima at 184.

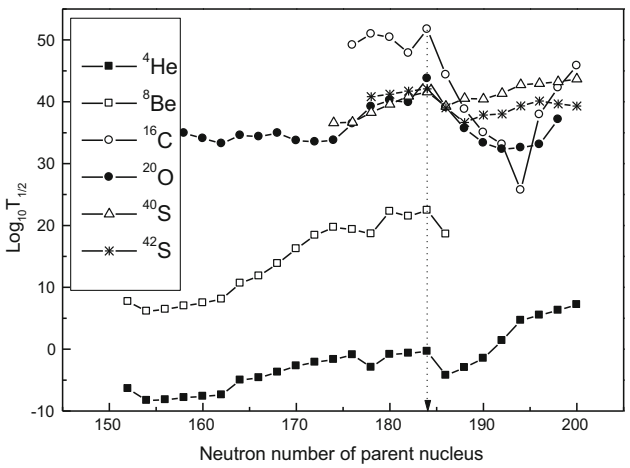

Figure 5. Computed half-life vs. neutron number of the parent nuclei for the parent $Z = 118$. The plots have the maxima at 184.

case of 114. In the same manner, the fact that two O nuclei-decay have the second-least half-life, has no significance as far as the daughter nuclei are concerned, as O nucleus contains magic proton number 8. The plot of half-life values against neutron number of the daughter nuclei shows a dip in the plot indicating that the corresponding neutron number is stable. A peak in the plot of half-life values against neutron number of the parent nuclei indicates that the corresponding neutron number is stable (or, daughter minima and parent maxima carry the same meaning). This idea is used to decipher the shell closures or the magic numbers. When half-lives of the cluster decays are plotted against neutron number of the daughter nuclei, it has been found that, minima occur at neutron number 184, for the clusters ^{4}He, ^{10}Be, ^{14}C, ^{16}C, ^{18}C, ^{22}O (figure 4). When half-lives of the cluster decays are plotted against neutron number of the parent nuclei, it has been found that, maxima occur at neutron number 184, for the clusters ^{4}He, ^{8}Be, ^{16}C, ^{20}O, ^{40}S, ^{42}S (figure 5). 184 has the maximum number of the daughter minima (six) and the parent maxima (six). This indicates that 184 neutrons make very strong combination. One can infer that there occurs shell closure at neutron number 184 or 184 is a magic neutron number. Zhang *et al* using GLDM [32], showed spherical shell closure at $N = 184$. Santhosh and Biju [33], using mass parabola method, also showed shell closure at $N = 184$.

Decays in which daughter nucleus has constant neutron number 184 (i.e., isotonic daughter nucleus having $N_1 = 184$) and varying proton number are now considered (table 5). The clusters ^{4}He, ^{14}C, ^{10}Be, ^{16}C, ^{22}O, ^{18}C have minimum half-lives associated with their decay when decayed to isotonic daughters having $N_1 = 184$, from various parents. Of these 'minimum half-lives', the one associated with ^{4}He has got the least value. In this case, the cluster has 2 each protons and neutrons and daughter has 116 protons. 2 being related to shell closure, this least 'minimum half-life' is to be considered as the result of shell closures in 2's and not to shell closure in 116 protons. The second-least 'minimum half-life' value is for that decay in which the cluster has 8 neutrons and daughter has 112 protons. 8 being related to shell closure, the second-leastness is to be attributed to shell closure in 8 and not to shell closure in 112 protons. The third-least 'minimum half-life' occurs for ^{10}Be decay. In^{10}Be neither proton nor neutron has shell closure. Therefore, this is the decay having the least 'minimum half-life' with clusters having general (non-magic) number of protons and neutrons. This leastness can be attributed to the proton shell closure in the daughter. In the daughter, proton number is 114. Hence, at 114 proton shell closure occurs (other decays, where proton numbers of the daughters are 112, 110 etc., have higher 'minimum half-life' values) (see figure 6)

The clusters ^{16}C, ^{20}O, ^{42}S, ^{40}S, ^{8}Be and ^{4}He have maximum half-lives associated with their decays when decayed from the parent ^{302}118 (compared to the decay from other parents) indicating shell closure at neutron number 184 (table 6). Of these 'maximum half-lives', the one associated with ^{4}He has the least value. But in this case, the cluster has 2 each protons and neutrons, 2 being a magic one. Therefore, the leastness is to be attributed to the magicity of 2; hence shell closure cannot be attributed to proton number 116 (of the daughter nucleus). The second-least 'maximum half-life' value has got to ^{8}Be-decay. This decay can be considered to possess the least 'maximum half-life' with cluster having general (non-magic) number of protons and neutrons. In this, daughter has proton number 114. This

Table 5. Variation of 'minimum half-life' with atomic number of isotonic daughters ($N_1 = 184$). Among the general (non-magic) clusters, the least value of 'minimum half-life' is associated with ^{10}Be-decay. This indicates proton shell closure at $Z = 114$.

Cluster	Parent for which one minimum occurs	Atomic number of the daughter Z_1	Neutron number of the parent N_1	$\log_{10}T_{1/2}$ (s)
^{4}He	^{304}118	116	184	−4.24
^{14}C	^{310}118	112	184	20.47
^{10}Be	^{308}118	114	184	22.96
^{16}C	^{312}118	112	184	25.74
^{22}O	^{316}118	110	184	31.55
^{18}C	^{314}118	112	184	50.45

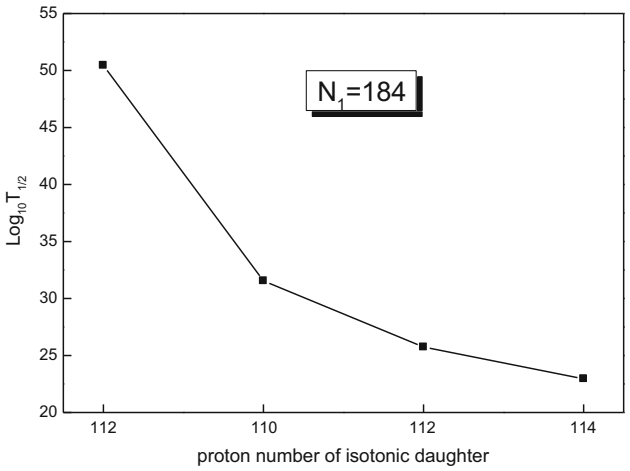

Figure 6. Variation of 'minimum half-life' with proton number of isotonic daughters ($N_1 = 184$). Least value occurs at $Z = 114$ indicating shell closure there.

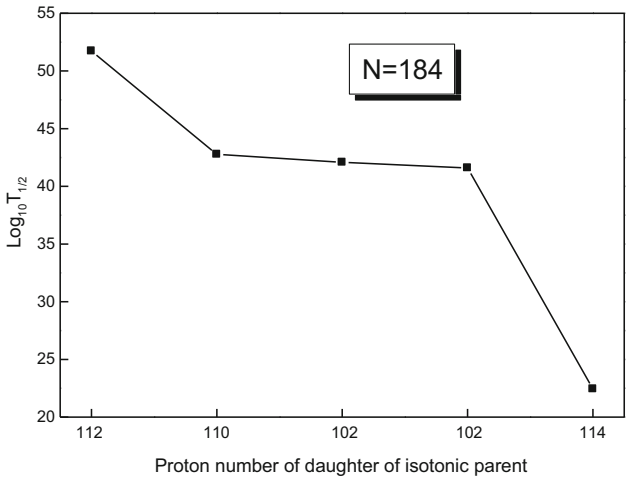

Figure 7. Variation of 'maximum half-life' of isotonic parent ($N = 184$) with proton number of daughters. For general (non-magic) clusters, least value occurs at $Z = 114$, indicating shell closure there.

leastness indicates proton shell closure at 114. (All other decays associated with 'maximum half-life', which have got proton number other than 114, namely, 112, 110, 102 in their daughter nuclei, have larger 'maximum half-life' values) (see figure 7)

In the case of emission of ^{10}Be, half-life reduces from ^{300}118, reaches a minimum at ^{308}118 and then increases, at least, upto ^{318}118, the last isotope considered. This indicates that stability of daughter nucleus increases from ^{290}114, reaches a maximum at ^{298}114 and then reduces, at least, upto ^{308}114, the daughter nuclei of the last isotope considered. This mainly indicates that when $N = 184$, there is a shell closure; this also indicates that the nuclide ^{298}114 can exist and is very stable. Thus, a very stable nuclide having proton number 114 and neutron number 184, viz., $^{298}_{184}$114 is seen in a natural manner in the superheavy region.

4. Summary and conclusion

Concepts of QMFT and cluster decay are used and shell closure of protons, with emphasis of superheavy region, has been found. As a part of getting information, half-lives are calculated. Rather than using an individual half-life as such, the relationship between them is used for finding shell closures. Neutron shell closure is found to occur at $N = 184$. Using this as the base step, $Z = 114$ is found to be the proton shell closure in the superheavy region. Also, combination of the above result with ^{10}Be-decay result, indicated that $^{298}_{184}$114 is a good candidate at the centre of island of stability. Our result is more in tune with the results from self-consistent mean-field theory, which predicted that double closed shell nucleus is with $Z = 114$, 120, 126 and $N = 184$ [7–9]; and not with the results that indicate the next double closed nucleus to be the sole one with $Z = 126$ and $N = 184$.

Table 6. Variation of 'maximum half-life' of isotonic parent ($N = 184$) with atomic number of the daughter. Among the general (non-magic) clusters, the least value of 'maximum half-life' is associated with ^{8}Be. This indicates proton shell closure at $Z = 114$.

Cluster	Parent for which one maximum occurs	Atomic number of the daughter Z_1	Neutron number of the parent N_1	$\log_{10}T_{1/2}$ (s)
^{16}C	^{302}118	112	184	51.72
^{20}O	^{302}118	110	184	42.77
^{42}S	^{302}118	102	184	42.08
^{40}S	^{302}118	102	184	41.60
^{8}Be	^{302}118	114	184	22.44
^{4}He	^{302}118	116	184	−0.36

It is a known fact that the higher is the neutron and proton shell closure values, the larger is the 'distance' to subsequent neutron and proton shell closure values. Hence, if neutron number 184 is unequivocally accepted to have shell closure, and, if $^{298}_{184}$114 is very stable, then, it can be inferred that there is no other very stable nuclide near $^{298}_{184}$114, having closed proton shell and neutron number 184; and $^{298}_{184}$114 itself is at the centre of island of stability. Nevertheless, it is probable that less strong proton closure is there at Z =120 or 126, and the corresponding nuclides of both carry far more higher number of neutrons than 184. One might be tempted to work, in the mode delineated here as well, until the centre of stability is decided to the fullest certainty.

References

[1] A Sandulescu, D N Poenaru and W Greiner, *Sov. J. Part. Nucl.* **II**, 528 (1980)

[2] R K Gupta, in: *Heavy elements and related new phenomena* edited by W Greiner and R K Gupta (World Scientific Publishers, Singapore, 1999) Vol. I, p. 536

[3] H J Rose and G A Jones, *Nature (London)* **307**, 245 (1984)

[4] D N Poenaru, Y Nagame, R A Gherghescu and W Greiner, *Phys. Rev. C* **65**, 054308 (2002); *Phys. Rev. C* **66**, 049902(E) (2002) and references therein.

[5] W D Myers and W J Swiatecki, *Nucl. Phys. A* **81**, 1 (1966)

[6] S K Patra, R K Gupta and W Greiner, *Mod. Phys. Lett. A* **12**, 1277 (1967)

[7] P Moller and R Nix, *J. Phys. G: Nucl. Part. Phys.* **20**, 1681 (1994)

[8] S Cwiok, J Dobaczewski, P H Heenen, P Magierski and W Nazarewicz, *Nucl. Phys. A* **611**, 211 (1996)

[9] M Bender, K Rutz, P G Reinhard and J A Maruhn, *Eur. Phys. J. A* **7**, 467 (2000)

[10] Y K Gambhir, A Bhagwat, M Gupta and A K Jain, *Phys. Rev. C* **68**, 044316 (2003)

[11] K P Santhosh and A Joseph, *Pramana – J. Phys.* **55**, 375 (2000)

[12] K P Santhosh and A Joseph, *Pramana – J. Phys.* **58**, 611 (2002)

[13] K P Santhosh and A Joseph, *Ind. J. Pure Appl. Phys.* **42**, 806 (2004)

[14] K P Santhosh and A Joseph, *Pramana – J. Phys.* **62**, 957 (2004)

[15] J Blocki, J Randrup, W J Swiatecki and C F Tsang, *Ann. Phys. (N.Y.)* **105**, 427 (1977)

[16] J Blocki and W J Swiatecki, *Ann. Phys. (N.Y.)* **132**, 53, (1981)

[17] D N Poenaru, M Ivascu, A Sandulescu and W Greiner, *Phys. Rev. C* **32**, 572 (1985)

[18] G Audi and A H Wapstra, *Nucl. Phys. A* **595**, 409 (1995)

[19] H Koura, T Tachibana, M Uno and M Yamada, *Prog. Theor. Phys.* **113**, 305 (2005)

[20] P Moller, J R Nix, W D Myers and W J Swiatecki, *At. Data Nucl. Data Tables* **59**, 185 (1995)

[21] Y J Shi and W J Swiatecki, *Nucl. Phys. A* **438**, 450 (1985)

[22] S S Malik and R K Gupta, *Phys. Rev. C* **39**, 1992 (1989)

[23] R K Gupta and W Greiner, *Int. J. Mod. Phys. E* **3**, 335 (1994)

[24] Yu Ts Oganessian, V K Utyonkov, Yu V Lobanov, F Sh Abdullin, A N Polyakov, R N Sagaidak, I V Shirokovsky, Yu S Tsyganov, A A Voinov, G G Gulbekian, S L Bogomolov, B N Gikal, A N Mezentsev, S Iliev, V G Subbotin, A M Sukhov, K Subotic, V I Zagrebaev, G K Vostokin, M G Itkis, K J Moody, J B Patin, D A Shaughnessy, M A Stoyer, N J Stoyer, P A Wilk, J M Kenneally, J H Landrum, J F Wild and R W Lougheed, *Phys. Rev. C* **74**, 044602 (2006)

[25] Yu Ts Oganessian, V K Utyonkov, Yu V Lobanov, F Sh Abdullin, A N Polyakov, I V Shirokovsky, Yu S Tsyganov, G G Gulbekian, S L Bogomolov, B N Gikal, A N Mezentsev, S Iliev, V G Subbotin, A M Sukhov, A A Voinov, G V Buklanov, K Subotic, V I Zagrebaev, M G Itkis, J B Patin, K J Moody, J F Wild, M A Stoyer, N J Stoyer, D A Shaughnessy, J M Kenneally, P A Wilk, R W Lougheed, R I Il'kaev and S P Vesnovskii, *Phys. Rev. C* **70**, 064609 (2004)

[26] M Bhuyan, S K Patra, B B Singh and R K Gupta, in *Proceedings of the International Symposium on Nuclear*

Physics edited by R K Choudhary, A K Mohanty, A Saxena, K Mahata and S Santra (India, 2009) Vol. 54, p. 182

[27] P Moller, J R Nix and K L Kratz, *At. Data Nucl. Data Tables* **66**, 131 (1997)

[28] J P Cui, Y L Zhang, S Zhang and Y Z Wang, *Phys. Rev. C* **97**, 014316 (2018)

[29] N Wang, M Liu, X Z Wu and J Meng, *Phys. Lett. B* **734**, 215 (2014)

[30] M Sayahi, V Dehghani, D Naderi and S A Alavi, *Z. Naturforsch. A* **74**, 551 (2019)

[31] R K Gupta, S Kumar, R Kumar, M Balasubramaniam and W Scheid, *J. Phys. G: Nucl. Part. Phys*. **28**, 2879 (2002)

[32] H Zhang, W Zuo, J Li and G Royer, *Phys. Rev. C* **74**, 017304 (2006)

[33] K P Santhosh and R K Biju, *Pramana – J. Phys.* **72**, 702 (2009)